# Group Consensus in Multilayer Networks

Francesco Sorrentino, Member, IEEE, Louis Pecora, and Ljiljana Trajković, Fellow, IEEE

Abstract—While there has been considerable work addressing consensus and group consensus in single-layer networks, not much attention has been devoted to consensus in multilayer networks. In this paper, we fill this gap by considering multilayer networks consisting of agents of different types while agents of the same type are arranged in separate layers. The patterns of emerging group consensus are determined by the symmetries of the multilayer network. An analysis of these symmetries reveals a partition of the nodes in each layer into clusters where the nodes in each cluster may achieve group consensus. We show that it is possible for group consensus to arise independently of the particular dynamics of the agents, which may be stable, marginally stable, or unstable. The concept of isolated group consensus where certain clusters of nodes in the multilayer network achieve group consensus while others do not is also introduced.

Index Terms—Consensus multilayer networks.

### I. INTRODUCTION AND BACKGROUND

RECENT research results considered the ability of a network to achieve group consensus where only groups of agents may reach consensus. In this context, studies have focused on either group consensus [1]–[6], cluster consensus [7]–[9], or multiconsensus [10]–[14]. In this paper, we consider group consensus. Results dealing with group (cluster) synchronizations of networks have been also reported [15]–[18]. Several papers [19]–[22] considered a specific structure of the network connectivity (both the inter-connectivity between groups and the intra-connectivity within each group) that enables group consensus, In this paper, the final group consensus is achieved as an emergent property of the network topology in terms of the network symmetries. The role of the networks symmetries in determining group consensus has been investigated in the context of single-layer networks [23].

Multilayer networks have recently received considerable attention in the research community [24], [25]. Epidemic dynamics [26]–[29] and collective behavior [30] in multilayer networks have been addressed as well as the spread of failures through

Manuscript received September 23, 2019; revised November 11, 2019; accepted November 12, 2019. Date of publication January 21, 2020; date of current version September 2, 2020. This work was supported by the Natural Sciences and Engineering Research Council of Canada under Grant 216844-13, by the Office of Naval Research through the Naval Research Laboratory's Basic Research Program, and by the US National Science Foundation under Grants CMMI- 1727948 and CRISP- 1541148. Recommended for acceptance by G. Yan. (Corresponding author: Francesco Sorrentino.)

- F. Sorrentino is with the University of New Mexico, Albuquerque, NM 87131 USA (e-mail: fsorrent@unm.edu).
- L. Pecora is with the Naval Research Laboratory, Code 6392, Washington, DC 20375 USA (e-mail: louis.pecora@nrl.navy.mil).
- L. Trajković is with the Simon Fraser University, Vancouver, BC V5A1S6, Canada (e-mail: ljilja@sfu.ca).

Digital Object Identifier 10.1109/TNSE.2020.2968436

interdependent networks [31]–[33]. Centrality measures that appropriately describe nodes of multilayer networks [34] and synchronization in multilayer networks have been investigated [35]–[41]. However, the emergence of consensus in multilayer networks has received little attention with few exceptions [42], [43] and a recent work focusing on opinion dynamics [44].

In this paper, we consider a network consisting of distinct layers where each layer is home to agents of a various *types* described by different uncoupled dynamics. Within the same layer, agents are connected through intra-layer connections while agents in different layers communicate through interlayer connections. We are interested in the emergence of group consensus where the agents within the same layer achieve consensus in clusters. For simplicity, we assume linear dynamics and study the pattern of consensus that emerges as a result of the specific intra-layer and inter-layer connectivity patterns. Our main result is the ability to predict agents within the same layer that will or will not achieve consensus based on the symmetries of the multilayer network.

# II. PRELIMINARIES

We first introduce notation that will be used throughout this paper. We denote with  $I_D$  the identity matrix of dimension D and with  $\mathbf{1}_D$  the column vector of length D whose entries are all ones. A group S is set S of elements with a defined binary operation that satisfies the following conditions: (i) closure: for each  $a,b\in S, ab\in S$ ; (ii) associativity: a(bc)=(ab)c for all  $a,b,c\in S$ ; (iii) existence of an identity element: S contains an element e such that ea=ae=a for every  $a\in S$ ; and (iv) existence of inverse elements: for every element  $a\in S$ , there exists an inverse element  $a^{-1}$  in S such that  $aa^{-1}=a^{-1}a=e$ . A nonempty subset of a group G is a subgroup G of G if it is itself a group with respect to the binary operation defined on G.

Definition 1: A coset of a subgroup  $\mathcal{H}$  of a group  $\mathcal{S}$  is defined as follows: Let  $\mathcal{H} = h_1, h_2, ..., h_m$  be a subgroup of a group  $\mathcal{S}$ . Then, for any a in  $\mathcal{S}$  the product  $a\mathcal{H} = ah_1, ah_2, ..., ah_m$  is called a left coset of  $\mathcal{H}$  in  $\mathcal{S}$  while the product  $\mathcal{H}a = h_1 a, h_2 a, ..., h_m a$  is called a right coset of  $\mathcal{H}$  in  $\mathcal{S}$ .

We next provide a definition for the symmetries of networks formed of a single layer where all nodes are of the same type [17], [45]. We define the symmetries of a multilayer network formed of several layers and agents of different types in each layer.

Definition 2: Each individual network layer  $\alpha$  is described by a graph  $\mathcal{G}^{\alpha}(\mathcal{V}(\mathcal{G}^{\alpha}),\mathcal{E}(\mathcal{G}^{\alpha}))$ , where the set of nodes  $\mathcal{V}(\mathcal{G}^{\alpha})=\{1,\ldots,N^{\alpha}\},\ |\mathcal{V}|=N^{\alpha}$  and a set of edges  $\mathcal{E}(\mathcal{G}^{\alpha})\subseteq\mathcal{V}\times\mathcal{V}$  where  $(i,j)\in\mathcal{E}$  if node j is connected to node i and  $(i,j)\notin\mathcal{E}$  otherwise. A permutation of the graph  $\pi(\mathcal{G}^{\alpha})=\mathcal{G}^{\alpha'}$  is an

2327-4697 © 2020 IEEE. Personal use is permitted, but republication/redistribution requires IEEE permission. See https://www.ieee.org/publications/rights/index.html for more information.

operation that: (i) permutes the nodes of the graph,  $\pi(i) = j$ ,  $i \in \mathcal{V}(\mathcal{G}^{\alpha})$ ; (ii) leaves the set of nodes unaltered  $\mathcal{V}(\mathcal{G}^{\alpha}) = \mathcal{V}(\mathcal{G}^{\alpha'})$ ; and (iii) associates to each edge  $(i,j) \in \mathcal{E}(\mathcal{G}^{\alpha})$  an edge  $(\pi(i),\pi(j)) \in \mathcal{E}(\mathcal{G}^{\alpha'})$ . If  $\mathcal{G}^{\alpha} = \mathcal{G}^{\alpha'}$ , then the permutation  $\pi$  is an automorphism ("symmetry") of the graph. If  $\pi$  is an automorphism and if  $(i,j) \in \mathcal{E}(\mathcal{G}^{\alpha})$ , then  $(\pi(i),\pi(j)) \in \mathcal{E}(\mathcal{G}^{\alpha})$ . If  $(i,j) \notin \mathcal{E}(\mathcal{G}^{\alpha})$ , then  $(\pi(i),\pi(j)) \notin \mathcal{E}(\mathcal{G}^{\alpha})$ . The set of automorphisms with the composition operation forms the automorphism group  $\mathcal{S}^{\alpha}$  of layer  $\mathcal{G}^{\alpha}$ .

Definition 3: The set of nodes  $\mathcal{V}^{\alpha}$  from layer  $\alpha$  is partitioned into disjoint subsets of nodes that are mapped into each other by applying all the symmetries in  $\mathcal{S}^{\alpha}$ . We refer to such subsets of nodes as "orbits" of the automorphism group  $\mathcal{S}^{\alpha}$  or "clusters" of the layer  $\alpha$ :  $\mathcal{C}_1^{\alpha}$ ,  $\mathcal{C}_2^{\alpha}$ , ...,  $\mathcal{C}_K^{\alpha}$ ,  $\mathcal{C}_k^{\alpha} \neq \emptyset$ ,  $\mathcal{C}_k^{\alpha} \cap \mathcal{C}_l^{\alpha} = \emptyset$ ,  $k \neq l$ , and  $\bigcup_{k=1}^K \mathcal{C}_k^{\alpha} = \mathcal{V}^{\alpha}$ . Orbits (clusters) consist of only one node are called trivial orbits (clusters).

Definition 4: A representation of the symmetry group  $\mathcal{S}^{\alpha}$  associates a matrix to each element of the group. For each symmetry  $\pi(i)=j,\ i\in\mathcal{V}$ , a natural choice is a permutation matrix that has all zero entries except for ones placed in row i and column  $\pi(i),\ i\in\mathcal{V}$ . The representation group is a group whose elements are the matrices and whose binary operation is matrix multiplication.

Definition 5: An irreducible representation of a group S is a group representation that has no nontrivial invariant subspaces [46].

## III. DYNAMICAL MODEL

We now provide a general model for the time evolution of the agents in a multilayer network. The underlying assumption is that each node of the multilayer network is home to a dynamical agent. Therefore, the terms node and agent will be used interchangeably. The term node is used when describing the network while the term agent is used when describing the node dynamics. A multilayer network is composed of:

- Sets of nodes/agents  $\{X^{\alpha}, \alpha=1,\ldots,M\}$ , where each set forms a different layer of the multi-layer network. All  $N^{\alpha}$  agents in the same layer  $X^{\alpha}$  share the same type of uncoupled dynamics that we assume to be linear:  $\dot{\mathbf{x}}_{i}^{\alpha}=F^{\alpha}\mathbf{x}_{i}^{\alpha}, i=1,\ldots,N^{\alpha}, \mathbf{x}^{\alpha}\in\mathbb{R}^{n^{\alpha}}$ . The total number of nodes/agents in the multilayer network is  $N=\sum_{\alpha}N^{\alpha}$ .
- A set of different interactions or couplings between nodes/agents. We differentiate between intra-layer and inter-layer interactions. (1) The intra-layer interactions connect nodes within the same layer  $X^{\alpha}$ . They are represented by an adjacency matrix  $A^{\alpha\alpha}$ . The interaction is modeled in terms of a square  $n^{\alpha}$ -dimensional matrix  $H^{\alpha\alpha}$  while the strength of the interaction is tuned using parameter  $\sigma^{\alpha\alpha}$ . (2) The inter-layer interactions connect nodes in two different layers  $\alpha$  and  $\beta$ , where  $\alpha \neq \beta$ . They are represented by an  $N^{\alpha} \times N^{\beta}$  adjacency matrix  $A^{\alpha\beta}$ . The associated coupling is determined by the  $n^{\alpha} \times n^{\beta}$  matrix  $H^{\alpha\beta}$ , where  $\sigma^{\alpha\beta}$  is the associated coupling strength. We assume that the couplings are undirected and, therefore,  $A^{\alpha\alpha} = A^{\alpha\alpha^T}$ ,  $\alpha = 1, \ldots, M$  and  $A^{\alpha\beta} = A^{\beta\alpha^T}$ ,  $\alpha$ ,  $\beta = 1, \ldots, M$ .

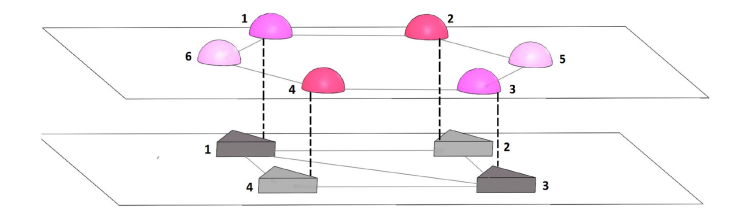


Fig. 1. A multilayer network with M=2 layers,  $N^1=6$  agents in layer 1 (top) and  $N^2=4$  agents in layer 2 (bottom). The agents in the top layer are of a different type than the agents in the bottom layer. Solid (dashed) lines are intra-layer (inter-layer) connections. Inside each layer, nodes in the same orbit (cluster) are of the same color.

An example of multilayer network consisting of M=2 layers,  $N^1=6$  nodes in layer 1, and  $N^2=4$  nodes in layer 2, is shown in Fig. 1.

For this network, the coupling matrices are:

$$A^{11} = \begin{bmatrix} 0 & 1 & 0 & 0 & 0 & 1 \\ 1 & 0 & 0 & 0 & 1 & 0 \\ 0 & 0 & 0 & 1 & 1 & 0 \\ 0 & 0 & 1 & 0 & 0 & 1 \\ 0 & 1 & 1 & 0 & 0 & 0 \\ 1 & 0 & 0 & 1 & 0 & 0 \end{bmatrix},$$

$$A^{12} = A^{21^{T}} = \begin{bmatrix} 1 & 0 & 0 & 0 \\ 0 & 1 & 0 & 0 \\ 0 & 0 & 1 & 0 \\ 0 & 0 & 0 & 1 \\ 0 & 0 & 0 & 0 \\ 0 & 0 & 0 & 0 \end{bmatrix},$$

$$A^{22} = \begin{bmatrix} 0 & 1 & 1 & 1 \\ 1 & 0 & 1 & 0 \\ 1 & 1 & 0 & 1 \\ 1 & 0 & 1 & 0 \end{bmatrix}.$$

$$(1)$$

The symmetry analysis shows that there are 3 clusters in layer 1:  $\mathcal{C}_1^{\alpha}=(1,3), \mathcal{C}_2^{\alpha}=(2,4), \mathcal{C}_3^{\alpha}=(5,6)$  and 2 clusters in layer 2:  $\mathcal{C}_1^{\beta}=(1,3), \mathcal{C}_2^{\beta}=(2,4)$ . Nodes in each layer that belong to the same orbit (cluster) have the same color.

We devise a model for the time evolution of each agent based on its individual dynamics and its connections to other agents through the connectivity of the multilayer network. Under the assumption that the overall effect of different interactions is equal to the sum of the individual interactions, the state  $\mathbf{x}_i(t)$  of agent i in layer  $\alpha$  of the multilayer network evolves based on linear equations:

$$\dot{\mathbf{x}}_{i}^{\alpha}(t) = F^{\alpha}\mathbf{x}_{i}^{\alpha}(t) + \underbrace{\sigma^{\alpha\alpha}\sum_{j=1}^{N^{\alpha}}A_{ij}^{\alpha\alpha}H^{\alpha\alpha}\mathbf{x}_{j}^{\alpha}(t)}_{\text{intra-layer couplings}} + \underbrace{\sum_{\beta\neq\alpha}\sigma^{\alpha\beta}\sum_{j=1}^{N^{\beta}}A_{ij}^{\alpha\beta}H^{\alpha\beta}\mathbf{x}_{j}^{\beta}(t)}_{\text{inter-layer couplings}},$$
(2)

 $i=1,\ldots,N^{\alpha}, \alpha=1,\ldots,M$ . We assume that  $F^{\alpha}\neq F^{\beta}$  as long as  $\alpha\neq\beta$ , where the superscript identifies *nodes of different types*. Furthermore,  $H^{\alpha\beta}\neq H^{\gamma\delta}$  as long as  $\alpha\neq\gamma$  and  $\beta\neq\delta$ , where the superscripts identify *interactions of different types*.

Equation (5) allows for an arbitrary number of layers M, an arbitrary number of nodes in each layer  $N^{\alpha}$ ,  $\alpha=1,\ldots,M$ , and arbitrary dimensions for the nodes in each layer  $n^{\alpha}$ ,  $\alpha=1,\ldots,M$ . We are interested in conditions for achieving group consensus where the nodes in each layer are divided into clusters and the nodes within the same cluster achieve group consensus but nodes between different clusters do not.

Each layer  $\alpha$  may be described by an intra-layer graph  $\mathcal{G}^{\alpha} = (\mathcal{V}^{\alpha}, \mathcal{E}^{\alpha})$  consisting of two sets:

- set of nodes  $\mathcal{V}^{\alpha} = \{i | i = 1, \dots, N^{\alpha}\}$  so that  $|\mathcal{V}^{\alpha}| = N^{\alpha}$ ,
- set of edges  $\mathcal{E}^{\alpha} = \subseteq \mathcal{V}^{\alpha} \times \mathcal{V}^{\alpha}$  where  $(i, j) \in \mathcal{E}^{\alpha}$  if node j is connected to node i and  $(i, j) \notin \mathcal{E}^{\alpha}$  otherwise.

The adjacency matrix of the intra-layer graph  $\mathcal{G}^{\alpha}$  is a binary matrix  $A^{\alpha\alpha} = \{A^{\alpha\alpha}_{ij}\} \in \mathbb{R}^{N^{\alpha} \times N^{\alpha}}$  such that element  $A^{\alpha\alpha}_{ij} = 1$  if  $(i,j) \in \mathcal{E}$  and  $A^{\alpha\alpha}_{ij} = 0$  if  $(i,j) \notin \mathcal{E}(\mathcal{G})$ . If  $\mathcal{G}^{\alpha}$  is undirected (directed), then  $A^{\alpha\alpha}$  is symmetric (non-symmetric).

Each pair of layers  $\alpha, \beta$  may be described by a bipartite inter-layer graph  $\mathcal{G}^{\alpha\beta} = (\mathcal{V}^{\alpha}, \mathcal{V}^{\beta}, \mathcal{E}^{\alpha\beta})$ , where  $\mathcal{E}^{\alpha\beta} = \subseteq \mathcal{V}^{\alpha} \times \mathcal{V}^{\beta}$  where  $(i,j) \in \mathcal{E}^{\alpha\beta}$  if node  $i \in \mathcal{V}^{\beta}$  is connected to node  $j \in \mathcal{V}^{\beta}$  and  $(i,j) \notin \mathcal{E}^{\alpha\beta}$  otherwise. The adjacency matrix  $\mathcal{G}^{\alpha\beta}$  of the inter-layer graph is a binary matrix  $A^{\alpha\beta} = \{A^{\alpha\beta}_{ij}\} \in \mathbb{R}^{N^{\alpha} \times N^{\beta}}$  such that element  $A^{\alpha\beta}_{ij} = 1$  if  $(i,j) \in \mathcal{E}^{\alpha\beta}$  and  $A^{\alpha\beta}_{ij} = 0$  if  $(i,j) \notin \mathcal{E}^{\alpha\beta}$ . In the case of undirected inter-layer connectivity,  $A^{\beta\alpha} = A^{\alpha\beta^T}$ .

Definition 6: The supra-adjacency matrix A is the  $\sum_{\alpha} N^{\alpha}$ -dimensional matrix:

$$A = \begin{bmatrix} A^{\alpha\alpha} & A^{\alpha\beta} & \dots \\ A^{\beta\alpha} & A^{\beta\beta} & \dots \\ \vdots & \vdots & \ddots \end{bmatrix}. \tag{3}$$

Since we have assumed that  $A^{\alpha\alpha}=A^{\alpha\alpha T}$  and  $A^{\beta\alpha}=A^{\alpha\beta T}$ , it follows that  $A=A^T$ .

#### IV. GROUP OF SYMMETRIES OF THE MULTILAYER NETWORK

We introduce here the group of symmetries of a multi-layer network. To analytically compute it, we first present a general form for the permutation matrices that represent the symmetries. Each network layer contains a different type of nodes and, hence, no permutation moves nodes between layers. This implies that the group of permutation symmetries  $\mathcal{S}$  for the entire network is block diagonal. For each permutation  $q \in \mathcal{S}$ :

$$g = \begin{pmatrix} g_{\alpha} & 0 & 0 & \dots \\ 0 & g_{\beta} & 0 & \dots \\ 0 & 0 & g_{\gamma} & \dots \\ \vdots & \vdots & \vdots & \ddots \end{pmatrix}, \tag{4}$$

where  $g_{\alpha}$  is the permutation that moves only nodes in layer  $\alpha$ ,  $g_{\beta}$  is the permutation that moves only nodes in layer  $\beta$ , etc.

Given the form (7), not every choice of  $g_{\alpha} \in \mathcal{S}^{\alpha}$ ,  $g_{\beta} \in \mathcal{S}^{\beta}$ , ... results in a symmetry for the multilayer network. For a

permutation matrix  $g \in \mathcal{S}$ , the symmetry group of the multilayer network should satisfy the following conditions:

$$g_{\alpha} \in \mathcal{S}^{\alpha}, \quad g_{\beta} \in \mathcal{S}^{\beta},$$
 (5a)

$$g_{\alpha}A^{\alpha\beta} = A^{\alpha\beta}g_{\beta}$$
 and  $g_{\beta}A^{\beta\alpha} = A^{\beta\alpha}g_{\alpha}$ , (5b)

$$\alpha, \beta = 1, ..., M, \quad \alpha \neq \beta.$$

The conjugacy relations (5b) is the requirement that permutations from different layers be *compatible* with the inter-layer coupling of the multi-layer network. We say that a permutation is *compatible* if it can be performed without changing the structure of the multilayer network. Hence, symmetries of the multilayer network will have the structure (4), where  $g_{\alpha} \in S^{\alpha}$ ,  $g_{\beta} \in S^{\beta}$ , ..., (5a). They also must satisfy the compatibility condition (5b) imposed by the inter-layer connectivity.

Consider an example of a multi-layer network with two layers  $\alpha$  and  $\beta$ . Equation (2) may be written as:

$$\dot{\mathbf{x}}^{\alpha} = I_{N^{\alpha}} \otimes F^{\alpha} \mathbf{x}^{\alpha} + \sigma^{\alpha \alpha} A^{\alpha \alpha} \otimes H^{\alpha \alpha} \mathbf{x}^{\alpha} + \sigma^{\alpha \beta} A^{\alpha \beta} \otimes H^{\alpha \beta} \mathbf{x}^{\beta}$$
$$\dot{\mathbf{x}}^{\beta} = I_{N^{\beta}} \otimes F^{\beta} \mathbf{x}^{\beta} + \sigma^{\beta \beta} A^{\beta \beta} \otimes H^{\beta \beta} \mathbf{x}^{\beta} + \sigma^{\beta \alpha} A^{\beta \alpha} \otimes H^{\beta \alpha} \mathbf{x}^{\alpha},$$

where the  $N^{\alpha}n^{\alpha}$ -dimensional vector  $\mathbf{x}^{\alpha} = [\mathbf{x}_1^{\alpha T}, \mathbf{x}_2^{\alpha T}, \ldots, \mathbf{x}_{N_{\alpha}}^{\alpha T}]^T$ , the  $N^{\beta}n^{\beta}$ -dimensional vector  $\mathbf{x}^{\beta} = [\mathbf{x}_1^{\beta T}, \mathbf{x}_2^{\beta T}, \ldots, \mathbf{x}_{N_{\beta}}^{\beta T}]^T$  and the symbol  $\otimes$  indicates the Kronecker product of matrices.

Consider two permutations  $g_{\alpha} \in \mathcal{S}^{\alpha}$  and  $g_{\beta} \in \mathcal{S}^{\beta}$ . From (7), a general element of the symmetry group for this two-layer network should be of the form:

$$\begin{pmatrix} g_{\alpha} & 0 \\ 0 & g_{\beta} \end{pmatrix}. \tag{6}$$

In order to determine compatible  $g_{\alpha}$  and  $g_{\beta}$ , we apply the two permutations to the full system dynamics,

$$\begin{split} g_{\alpha}\dot{\mathbf{x}}^{\alpha} &= I_{N^{\alpha}} \otimes F^{\alpha}g_{\alpha}\mathbf{x}^{\alpha} + \sigma^{\alpha\alpha}A^{\alpha\alpha} \otimes H^{\alpha\alpha}g_{\alpha}\mathbf{x}^{\alpha} \\ &+ \sigma^{\alpha\beta}g_{\alpha}A^{\alpha\beta} \otimes H^{\alpha\beta}\mathbf{x}^{\beta} \\ g_{\beta}\dot{\mathbf{x}}^{\beta} &= I_{N^{\beta}} \otimes F^{\beta}g_{\beta}\mathbf{x}^{\beta} + \sigma^{\beta\beta}A^{\beta\beta} \otimes H^{\beta\beta}g_{\beta}\mathbf{x}^{\beta} \\ &+ \sigma^{\beta\alpha}g_{\beta}A^{\beta\alpha} \otimes H^{\beta\alpha}\mathbf{x}^{\alpha}, \end{split}$$

where we have used the property that permutations commute with the intra-layer coupling matrices.

From (7), flow invariance requires that the conjugacy relations be satisfied:  $g_{\alpha}A^{\alpha\beta}=A^{\alpha\beta}g_{\beta}$  and  $g_{\beta}A^{\beta\alpha}=A^{\beta\alpha}g_{\alpha}$ . This implies that  $g_{\alpha}$  and  $g_{\beta}$  are not arbitrarily chosen and must be properly paired to satisfy (5b). Because there may not be a matching  $g_{\beta}$  for each  $g_{\alpha}$  and vice versa, the conjugacy relations will generally restrict the permitted permutations to subgroups of  $S^{\alpha}$  and  $S^{\beta}$ . It is the structure of these subgroups that will determine the final group S of the entire network.

To find the permutations that satisfy the conjugacy relations (8b), we define the following sets:

$$\mathcal{H}^{\alpha} = \{ g_{\alpha} \in \mathcal{S}^{\alpha} | g_{\alpha} A^{\alpha\beta} = A^{\alpha\beta} g_{\beta} \text{ and } g_{\beta} A^{\beta\alpha} = A^{\beta\alpha} g_{\alpha}$$
 (7)

for some  $g_{\beta} \in \mathcal{S}^{\beta}$  and

$$\mathcal{H}^{\beta} = \{ g_{\beta} \in \mathcal{S}^{\beta} | g_{\beta} A^{\beta \alpha} = A^{\beta \alpha} g_{\alpha} \text{ and } g_{\alpha} A^{\alpha \beta} = A^{\alpha \beta} g_{\beta}$$
 (8)

for some  $g_{\alpha} \in \mathcal{S}^{\alpha}$ . A proof that  $\mathcal{H}^{\alpha}$  is a subgroup of  $\mathcal{S}^{\alpha}$  and  $\mathcal{H}^{\beta}$ 

is a subgroup of  $\mathcal{S}^{\beta}$  can be found in [47], [48]. Note that  $A^{\alpha\beta} \in \mathbb{R}^{N^{\alpha} \times N^{\beta}}$ , while an element  $g_{\alpha} \in \mathcal{H}^{\alpha}$  may be represented with a  $N^{\alpha} \times N^{\alpha}$  matrix and an element  $g_{\beta} \in \mathcal{H}^{\beta}$  may be represented with a  $N^{\beta} \times N^{\beta}$  matrix. It follows from this observation that  $A^{\alpha\beta}$  has generally nontrivial left and right null spaces (with no particular structure) and, hence, there may be more than one  $g_{\alpha}$  that satisfies  $g_{\alpha}A^{\alpha\beta} = A^{\alpha\beta}g_{\beta}$  for a given  $g_{\beta}$  and vice versa.

We next show how the group of symmetries of the multilayer network S can be obtained from  $\mathcal{H}^{\alpha}$  and  $\mathcal{H}^{\beta}$ . To properly pair the permutations, we introduce an equivalence relation on each subgroup  $\mathcal{H}^{\alpha}$  and  $\mathcal{H}^{\beta}$ . We define a relation  $\sim$  between the elements of  $\mathcal{H}^{\alpha}$  as  $g \sim g'$  if  $gA^{\alpha\beta} = g'A^{\alpha\beta}$ . Similarly,  $h \sim h'$  if  $hA^{\beta\alpha} = h'A^{\beta\alpha}$ . Because relation  $\sim$  is defined using equalities, it is an equivalence relation (reflexive, symmetric, and transitive) on  $\mathcal{H}^{\alpha}$  and  $\mathcal{H}^{\beta}$ . Moreover, if  $g \sim g'$ , g, and h are conjugate, then so are g' and h. This implies that the relation defines a disjoint partitioning of each subgroup into subsets,  $\mathcal{K}_i^{\alpha}$  and  $\mathcal{K}_i^{\beta}$ ,  $i=1,\ldots,K$  for  $\mathcal{H}^{lpha}$  and  $\mathcal{H}^{eta}$ , respectively. Each subset  $\mathcal{K}^{lpha}_i$  contains all permutations g such that  $gA^{\alpha\beta}$  is equal to a certain matrix  $M_i$ . Correspondingly, each subset  $\mathcal{K}_i^{\beta}$  contains all permutations h such that  $hA^{\beta\alpha} = M_i$ . This leads to the construction of the group of symmetries of the multilayer network S as:

$$S = \left\{ \begin{pmatrix} g_{\alpha} & 0 \\ 0 & g_{\beta} \end{pmatrix} | g_{\alpha} \in \mathcal{K}_{i}^{\alpha} \text{ and } g_{\beta} \in \mathcal{K}_{i}^{\beta}, \text{ for } i = 1, ..., Z \right\}.$$
(9)

Note that the sets  $\mathcal{K}_i^{\alpha}$  and  $\mathcal{K}_i^{\beta}$  may contain different number of

*Remark 1:* For each layer  $\alpha$ , the sets  $\mathcal{K}_i^{\alpha}$  form cosets for the layer's subgroup  $\mathcal{H}^{\alpha}$  [47]. It suffices to notice that one of the  $\mathcal{K}_i^{\alpha}$  subsets that contains the identity symmetry is a subgroup of  $\mathcal{H}^{\alpha}$ . If  $\mathcal{K}^{\alpha}_1$  is the subgroup, it follows that all  $\mathcal{K}^{\alpha}_i$  are left and right cosets of  $\mathcal{K}_1^{\alpha}$ .

It is now possible to define the orbits of the symmetry group S. Each orbit is formed of the nodes of the multilayer network that are mapped into each other when all the symmetry operations of the group S are applied. Because there are no symmetry operations that swap nodes between different layers, all the orbits are formed by nodes in the same layer.

Definition 7: The symmetry group S partitions the nodes of the multilayer network into orbits. As a result, the nodes in each layer  $\alpha$  are partitioned into clusters  $C_k^{\alpha}$ ,  $k=1,\ldots,L^{\alpha}$ , each consisting of the nodes in orbit k and  $\bigcup_{k=1}^{L^{\alpha}} \mathcal{C}_{k}^{\alpha} = \mathcal{V}^{\alpha}$ ,  $\alpha=1,..,M,$   $\mathcal{C}_{k}^{\alpha}\neq\emptyset$  and  $\mathcal{C}_{k}^{\alpha}\cap\mathcal{C}_{l}^{\alpha}=\emptyset,$   $k\neq l.$ 

Let  $N_k^{\alpha} = |\mathcal{C}_k^{\alpha}|$  denote the number of nodes of layer  $\alpha$  in orbit k and  $\sum_{k=1}^{q} N_k^{\alpha} = N^{\alpha}$ . For simplicity and without loss of generality, we assume that nodes in each layer  $\alpha$  are numbered corresponding to their orbits. For example, nodes in orbit 1 are labeled  $1, \ldots, N_1^{\alpha}$  while nodes in orbit 2 are labeled  $N_1^{\alpha}$  +  $1, \ldots, N_1^{\alpha} + N_2^{\alpha}$ . Then, each matrix  $A^{\alpha\beta}$  may be rewritten as:

$$A^{\alpha\beta} = \begin{bmatrix} A^{\alpha\beta}_{\ell\ell} & A^{\alpha\beta}_{\ell k} & \cdots \\ A^{\alpha\beta}_{k\ell} & A^{\alpha\beta}_{kk} & \cdots \\ \vdots & \vdots & \ddots \end{bmatrix}, \tag{10}$$

where the  $N_\ell^{\alpha} \times N_k^{\beta}$  block  $A_{\ell k}^{\alpha\beta}$  denotes the coupling between cluster  $\ell$  in layer  $\alpha$  k and cluster  $\ell$  in layer  $\alpha$ .

## V. GROUP CONSENSUS IN MULTI-LAYER NETWORKS WITH LINEAR DYNAMICS

The time evolution of each layer of the multilayer network is described as:

$$\dot{\mathbf{x}}^{\alpha}(t) = I_{N^{\alpha}} \otimes F^{\alpha} \mathbf{x}^{\alpha}(t) + \sum_{\beta=1}^{M} A^{\alpha\beta} \otimes \hat{H}^{\alpha\beta} \mathbf{x}^{\beta}(t) \qquad \alpha = 1, ..., M,$$
(11)

in the  $N^{\alpha}m^{\alpha}$ -dimensional vector  $\mathbf{x}^{\alpha} = [\mathbf{x}_{1}^{\alpha}(t)^{T}, \mathbf{x}_{2}^{\alpha}(t)^{T}, \ldots, \mathbf{x}_{N^{\alpha}}^{\alpha}(t)^{T}]^{T}$ ,  $\alpha = 1, \ldots, M$ , where  $\hat{H}^{\alpha\beta} = \sigma^{\alpha\beta}H^{\alpha\beta}$ .

A global system of equations describing the time evolution of the entire multilayer network can be written by introducing the  $P = \sum_{\alpha} N^{\alpha} n^{\alpha}$ -dimensional vector  $\mathbf{x}(t) = [\mathbf{x}^{1}(t)^{T}, \mathbf{x}^{2}(t)^{T}, \dots,$ 

$$\dot{\mathbf{x}}(t) = \begin{pmatrix}
I_{N^{\alpha}} \otimes F^{\alpha} & 0 & \cdots \\
0 & I_{N^{\beta}} \otimes F^{\beta} & \cdots \\
\vdots & \vdots & \ddots
\end{pmatrix} \\
+ \begin{pmatrix}
A^{\alpha\alpha} \otimes \hat{H}^{\alpha\alpha} & A^{\alpha\beta} \otimes \hat{H}^{\alpha\beta} & \cdots \\
A^{\beta\alpha} \otimes \hat{H}^{\beta\alpha} & A^{\beta\beta} \otimes \hat{H}^{\beta\beta} & \cdots \\
\vdots & \vdots & \ddots
\end{pmatrix} \mathbf{x}(t) = \mathbf{\Xi}\mathbf{x}(t), \tag{12}$$

where the P-dimensional square matrix  $\Xi$  has eigenvalues  $\xi_{\ell}$ ,  $\ell = 1, ..., P.$ 

Definition 8: The set of states  $\mathbf{x}_i^{\alpha} = \mathbf{x}_i^{\alpha}$  if i and j lie in the same orbit  $C_k^{\alpha}$ ,  $\alpha = 1, ..., M, k = 1, ..., \mathring{L}^{\alpha}$  define an invariant manifold called the group consensus manifold.

The dynamics on the group consensus manifold is governed by the *quotient network* dynamics [23]:

$$\dot{\mathbf{q}}_{k}^{\alpha}(t) = F^{\alpha}\mathbf{q}_{k}^{\alpha}(t) + \sum_{\beta} \sum_{l} Q_{kl}^{\alpha\beta} \hat{H}^{\alpha\beta}\mathbf{q}_{l}(t), \quad k = 1, \dots, L^{\alpha},$$
(13)

where  $\mathbf{q}_k^{\alpha}(t)$  is now the state of orbit  $k=1,\ldots,L^{\alpha}$  in layer  $\alpha$  and the  $L^{\alpha}\times L^{\beta}$  matrix  $Q^{\alpha\beta}$  has entries  $Q_{kl}^{\alpha\beta}=\sum_j A_{ij}^{\alpha\beta}$  for  $i \in \mathcal{C}^{\alpha}$  and  $j \in \mathcal{C}^{\beta}$ . Equivalently:

$$\dot{\mathbf{q}}(t) = \begin{pmatrix} \begin{bmatrix} I_{L^{\alpha}} \otimes F^{\alpha} & 0 & \cdots \\ 0 & I_{L^{\beta}} \otimes F^{\beta} & \cdots \\ \vdots & \vdots & \ddots \end{bmatrix} \\ + \begin{bmatrix} Q^{\alpha\alpha} \otimes \hat{H}^{\alpha\alpha} & Q^{\alpha\beta} \otimes \hat{H}^{\alpha\beta} & \cdots \\ Q^{\beta\alpha} \otimes \hat{H}^{\beta\alpha} & Q^{\beta\beta} \otimes \hat{H}^{\beta\beta} & \cdots \\ \vdots & \vdots & \ddots \end{bmatrix} \mathbf{q}(t) = \Psi \mathbf{q}(t),$$
(14)

in the  $R = \sum_{\alpha} L^{\alpha} n^{\alpha}$ -dimensional vector  $\mathbf{q}(t) = [\mathbf{q}^1(t)^T, \mathbf{q}^2(t)^T, \ldots, \mathbf{q}^M(t)^T]^T$  and each vector  $\mathbf{q}^i(t) = [\mathbf{q}^i_1(t)^T, \mathbf{q}^i_2(t)^T, \ldots, \mathbf{q}^i_{I^i}(t)^T]^T$ .

We now introduce the square  $L = \sum_{\alpha} L^{\alpha}$ -dimensional matrix Q defined as:

$$Q = \begin{bmatrix} Q^{\alpha\alpha} & Q^{\alpha\beta} & \dots \\ Q^{\beta\alpha} & Q^{\beta\beta} & \dots \\ \vdots & \vdots & \ddots \end{bmatrix}. \tag{15}$$

It is related to the matrix A by the following relation:

$$Q = (E^{T}E)^{-1}E^{T}AE = E^{\dagger}AE,$$
 (16)

where E is the  $N \times L$  indicator matrix  $E_{ij}$  equal to 1 if node i is in orbit j and is 0 otherwise [49].

Remark 2: The matrix  $E = \bigoplus_{\alpha=1}^{M} \bigoplus_{k=1}^{L^{\alpha}} \mathbf{1}_{N_{k}^{\alpha}}$ , where the symbol  $\oplus$  indicates the direct sum operation.

Remark 3: The quotient network vector  $\mathbf{q}(t) = (E'^T E')^{-1}$  $E'^T \mathbf{x}(t)$ , where the  $R \times P$ -dimensional indicator matrix E' maps each state of the P-dimensional vector  $\mathbf{x}(t)$  to one and only one state of the quotient network R-dimensional vector  $\mathbf{q}(t)$ :  $E' = \bigoplus_{\alpha=1}^M \bigoplus_{k=1}^{L^{\alpha}} (I_{n_{\alpha}} \otimes \mathbf{1}_{N_k^{\alpha}})$ .

The quotient network describes the evolution of the agents on the group consensus manifold. In case when all the agents in the same cluster are given the same initial condition, the quotient network dynamics provides the exact time evolution of all network agents. The quotient network dynamics is stable in the group consensus manifold if the largest real part of the eigenvalues of the matrix  $\Psi$  defined in (14).

Under appropriate conditions, the set of equations (11) and (12) will admit group consensus. A set of agents may converge on group consensus on either a stable, unstable, or marginally stable trajectory. It is important to note that we are not concerned with whether or not the entire system is asymptotically stable. Instead, we address the stability of each agent with respect to the group consensus state where all nodes in its orbits have reached consensus.

Definition 9: Nodes in orbit  $\mathcal{C}_k^{\alpha}$  have achieved group consensus if  $\lim_{t\to\infty}\|\mathbf{x}_i^{\alpha}(t)-\mathbf{x}_j^{\alpha}(t)\|=0$  for all i and j in  $\mathcal{C}_k^{\alpha}$ . Hence, group consensus is possible for either stable, marginally stable, or unstable dynamics as long as the trajectories converge to each other.

Remark 4: In general, a study of the eigenvalues  $\xi_\ell$ ,  $\ell=1,\ldots,P$  is not sufficient to predict group consensus: (i) Only if all eigenvalues have a negative real part  $Re(\xi_\ell)<0$ ,  $\ell=1,\ldots,P$ , the set of equations converge on the group consensus manifold with all  $\lim_{t\to\infty} x_i^\alpha(t)=0$ . If for one or more eigenvalues  $Re(\xi_\ell)>0$ , it is difficult to predict whether or not group consensus is achieved unless one is able to determine whether those eigenvalues with positive real part correspond to motion parallel to the group consensus manifold or are transverse to it. In particular, if for one or more eigenvalues  $Re(\xi_\ell)>0$ , one of the following two cases may arise: (ii) group consensus is achieved on a diverging trajectory; or (iii) group consensus is not achieved.

The remainder of the paper is devoted to determining conditions when eigenvalues  $\xi_{\ell}$  are associated with motion parallel or orthogonal to the group consensus manifold. We use a transformation of the system dynamics provided by group theory in order to fully characterize stability of group consensus.

Based on the group of symmetries of the multilayer network, we may compute the irreducible representations (IRRs) of the symmetry group of the multilayer network. We define a transformation  $T^{\alpha}$  for each layer  $\alpha$  to the so called IRR coordinate system [17]. The global transformation of the multilayer network to the IRR coordinate system may be written as a block diagonal matrix with the direct sum of the transformations of each layer (the orthonormal matrix T),

$$T = \bigoplus_{\alpha} T^{\alpha}. \tag{17}$$

By construction, each row of the matrix  $T^{\alpha}$  is associated with a specific cluster  $\mathcal{C}_k^{\alpha}$ : all the i entries of that row of the matrix  $T^{\alpha}$  are zero for  $i \notin \mathcal{C}_k^{\alpha}$ .  $N_1^{\alpha}$  rows of the matrix  $T^{\alpha}$  are associated with cluster 1,  $N_2^{\alpha}$  rows are associated to cluster 2, .... For each matrix  $T^{\alpha}$ , the first  $L^{\alpha}$  rows satisfy  $T_{ki}^{\alpha} = 1/\sqrt{N_k^{\alpha}}$  if node  $i \in \mathcal{C}_k^{\alpha}$  and  $T_{ki} = 0$  otherwise. These rows describe motion that is parallel to the consensus manifold. The remaining rows describe motion that is orthogonal to the consensus manifold and, thus, determine its transverse stability. If one of these rows  $k = L^{\alpha} + 1, \ldots, N^{\alpha}$  is associated with cluster  $\mathcal{C}_k^{\alpha}$ ,  $\sum_{i \in \mathcal{C}_k^{\alpha}} T_{ki}^{\alpha} = 0$ .

We now construct the P-dimensional orthonormal matrix  $\tilde{T}$  that will be used to block-diagonalize (12):

$$\tilde{T} = \underset{\alpha}{\oplus} T^{\alpha} \otimes I_{n_{\alpha}}. \tag{18}$$

Application of the transformation  $\tilde{T}$  to (12) yields:

$$\dot{\mathbf{z}}(t) = \begin{pmatrix}
I_{N^{\alpha}} \otimes F^{\alpha} & 0 & \cdots \\
0 & I_{N^{\beta}} \otimes F^{\beta} & \cdots \\
\vdots & \vdots & \ddots
\end{pmatrix} \\
+ \begin{pmatrix}
B^{\alpha\alpha} \otimes \hat{H}^{\alpha\alpha} & B^{\alpha\beta} \otimes \hat{H}^{\alpha\beta} & \cdots \\
B^{\beta\alpha} \otimes \hat{H}^{\beta\alpha} & B^{\beta\beta} \otimes \hat{H}^{\beta\beta} & \cdots \\
\vdots & \vdots & \ddots
\end{pmatrix} \tilde{\mathbf{z}}(t), \quad (19)$$

where vector  $\tilde{\mathbf{z}}(t) = (\tilde{T} \otimes I_m)\mathbf{z}(t)$  and each block  $B^{\alpha\beta} = T^{\alpha}A^{\alpha\beta}T^{\beta^T}$ . It is important to note that application of the matrix  $\tilde{T}$  leaves the leftmost matrix on the right-hand side of (12) unaltered. (Compare with the leftmost matrix on the right hand side of (19).)

We also define the N-dimensional square matrix:

$$B = \begin{bmatrix} B^{\alpha\alpha} & B^{\alpha\beta} & \cdots \\ B^{\beta\alpha} & B^{\beta\beta} & \cdots \\ \vdots & \vdots & \ddots \end{bmatrix}, \tag{20}$$

that be computed as  $B = TAT^T$ . Moreover, after permutations of its rows and columns, the matrix B has a block-diagonal structure that is determined by the irreducible representation of the symmetry group of the multilayer network. Namely:

$$\Pi B \Pi^T = \bigoplus_{s=1}^S I_{d_s} \otimes \tilde{B}_s, \tag{21}$$

where  $\Pi$  is an appropriate permutation matrix,  $\tilde{B}_s$  is a (complex)  $p_s \times p_s$  matrix, with  $p_s$  the multiplicity of the sth IRR representation of the group, S is the number of IRRs, and  $d_s$  is the dimension of the sth IRR so that  $\sum_{s=1}^S d_s p_s = N$  [17]. The trivial representation (s=1) which describes the motion in the consensus manifold has  $p_1 = L$  and is associated with all the L clusters of the multilayer network. Each remaining representation  $s=2,\ldots,S$  is associated with either: (i) an individual cluster  $(p_s=1)$  or (ii) a set of intertwined clusters  $(p_s>1)$  [17].

By taking advantage of the block diagonal structure of (21), the vector  $\tilde{\mathbf{z}}(t)$  in (19) may be decomposed into S independently evolving vectors  $\tilde{\mathbf{z}}^T = [\tilde{\mathbf{z}}_1^T, \tilde{\mathbf{z}}_2^T, \dots, \tilde{\mathbf{z}}_S^T]$ , each corresponding to an irreducible representation  $s = 1, \dots, S$ . For each  $s = 1, \dots, S$ , an independent system  $\dot{\tilde{\mathbf{z}}}_s = \hat{B}_s \tilde{\mathbf{z}}_s(t)$  may be written. We first consider the case when  $p_s = 1$ . The corresponding system s satisfies:

$$\dot{\tilde{\mathbf{z}}}_s = (F^a + \tilde{B}_s \hat{H}^{aa}) \tilde{\mathbf{z}}_s, \tag{22}$$

where a is the layer of the cluster associated with the IRR s. In case  $p_s=2$ , there are two clusters a and b associated with the IRR. Hence, the corresponding system s satisfies,

$$\dot{\tilde{\mathbf{z}}}_s(t) = \begin{bmatrix} F^a + \tilde{B}_s^{aa} \otimes \hat{H}^{aa} & \tilde{B}_s^{ab} \otimes \hat{H}^{ab} \\ \tilde{B}_s^{ba} \otimes \hat{H}_s^{ba} & F^b + \tilde{B}^{bb} \otimes \hat{H}^{bb} \end{bmatrix} \tilde{\mathbf{z}}_s(t). \quad (23)$$

Similarly, one may write the systems s for  $p_s > 2$ . A special case is the trivial irreducible representation (s = 1), which is associated with all L network clusters  $(p_1 = L)$ .

An immediate consequence of the particular block-diagonal structure of the matrix B (24) is that the transformed state vector is partitioned into two independent vectors:  $\tilde{\mathbf{z}}(t) = [\tilde{\mathbf{z}}_{para}^T(t), \quad \tilde{\mathbf{z}}_{orth}^T(t)]^T$ , where  $\tilde{\mathbf{z}}_{para}(t) \equiv \tilde{\mathbf{z}}_1(t) \in \mathbb{R}^R$  describes the motion along the group consensus manifold and  $\tilde{\mathbf{z}}_{orth}(t) \equiv [\tilde{\mathbf{z}}_2(t)^T, \ldots, \tilde{\mathbf{z}}_S(t)^T]^T \in \mathbb{R}^{P-R}$  describes the motion orthogonal to the group consensus manifold:

$$\begin{bmatrix} \dot{\tilde{\mathbf{z}}}_{para}(t) \\ \dot{\tilde{\mathbf{z}}}_{orth}(t) \end{bmatrix} = \begin{bmatrix} \hat{B}_{para} & O_{(R \times P - R)} \\ O_{(P - R \times R)} & \hat{B}_{orth} \end{bmatrix} \begin{bmatrix} \tilde{\mathbf{z}}_{para}(t) \\ \tilde{\mathbf{z}}_{orth}(t) \end{bmatrix}. \quad (24)$$

We define  $\lambda_{para}$  and  $\lambda_{orth}$  to be the maximum real part of the eigenvalues of the matrices  $\hat{B}_{para}$  and  $\hat{B}_{orth}$ , respectively. An analogous derivation of (27) may be found in [49].

Theorem 1: Stability of the motion along (orthogonal to) the group consensus manifold is determined by the sign of  $\lambda_{para}$  ( $\lambda_{orth}$ ). Namely, the motion in the group consensus manifold decays to zero if and only if  $\lambda_{para} < 0$  ( $\hat{B}_{para}$  is Hurwitz). Group consensus is achieved if and only if  $\lambda_{orth} < 0$  ( $\hat{B}_{orth}$  is Hurwitz). In this case, the group consensus manifold is stable and any perturbation orthogonal to the group consensus manifold will decay to zero independent of the dynamics along the manifold.

*Proof:* The block diagonal structure of the matrix (27) shows that (17) decouples into two independent equations.

One needs to prove that these two equations correspond to motion parallel to the consensus manifold and motion parallel to it. This follows from the particular structure of the matrices  $T^{\alpha}$ ,  $\alpha=1,...,M$ . The vector  $\mathbf{x}(t)$  in (17) may be written as a linear combination of the components of the vectors  $\tilde{\mathbf{z}}_{para}(t)$  and  $\tilde{\mathbf{z}}_{orth}(t)$ . In particular for every two nodes i and j from the same cluster  $C_k^{\alpha}$ , the difference  $(\mathbf{x}_i^{\alpha}(t)-\mathbf{x}_j^{\alpha}(t))$  is a linear combination only of the components of the vector  $\tilde{\mathbf{z}}_{orth}(t)$ . Thus, the motion orthogonal to the group consensus manifold is  $\tilde{\mathbf{z}}_{orth}(t)$  and the motion parallel to the group consensus manifold is  $\tilde{\mathbf{z}}_{orth}(t)$ .

Theorem 1 implies that it is possible for the original system to be either marginally stable or unstable and yet achieve group consensus.

Remark 5: If the group consensus manifold is stable  $(\lambda_{para} < 0)$ , for large t,  $\mathbf{x}_i^{\alpha}(t)$  converges to  $\mathbf{q}_k^{\alpha}(t)$ ,  $i \in \mathcal{C}_k^{\alpha}$  and the full multilayer network dynamics is completely described by the quotient network dynamics. Then, the final group consensus state is equal to  $\mathbf{q}(\infty) = \lim_{t \to \infty} \exp(\Psi t) \mathbf{q}(0) = \lim_{t \to \infty} \exp(\Psi t) (E^{\prime T} E^{\prime})^{-1} E^{\prime T} \mathbf{x}(0)$ . This expression explains how the choice of the initial conditions determines the final group consensus state.

Theorem 2: The two matrices  $\Psi$  and  $\hat{B}_{para}$  are similar.

Proof: Recall the definitions of the matrices T (20) and  $\tilde{T}$  (18). For each matrix  $T^{\alpha}$ , the first  $L^{\alpha}$  rows satisfy  $T_{ki}^{\alpha} = \sqrt{N_k^{\alpha}}^{-1}$  if node i is in cluster k of layer  $\alpha$  and  $T_{ki} = 0$  otherwise. For each layer  $\alpha$ , we may construct the  $L^{\alpha} \times N^{\alpha}$  matrix  $T'^{\alpha}$  by stacking together the first  $L^{\alpha}$  rows of the matrix  $T^{\alpha}$ . We may then construct the  $R \times P$ -dimensional matrix  $T' = \bigoplus_{\alpha} T'^{\alpha} \otimes I_{n_{\alpha}}$ . From (27),  $\dot{\mathbf{z}}_{para}(t) = \hat{B}_{para} \dot{\mathbf{z}}_{para}(t)$ , where  $\dot{\mathbf{z}}_{para}(t) = T'\tilde{\mathbf{z}}(t)$ . By construction,  $T' = (E'E'^T)^{-\frac{1}{2}}E'$ . From (17),  $\dot{\mathbf{q}}(t) = \Psi\mathbf{q}(t)$ , where  $\mathbf{q}(t) = (E'E'^T)^{-1}E'\mathbf{x}(t) = (E'E'^T)^{-\frac{1}{2}}T'\mathbf{x}(t)$ . Hence,  $\mathbf{q}(t) = (E'E'^T)^{-\frac{1}{2}}\tilde{\mathbf{z}}_{para}(t)$  and  $\hat{B}_{para} = (E'E'^T)^{\frac{1}{2}}\Psi(E'E'^T)^{-\frac{1}{2}}$ .

Remark 6: From Theorem 2,  $\mathbf{q}(t) = (E'E'^T)^{-\frac{1}{2}}\tilde{\mathbf{z}}_{para}(t)$ . Hence, the quotient network dynamics (14) decays to zero if and only if  $\lambda_{para} < 0$ .

Based on the block-diagonal structure of matrix:

$$\hat{B}_{orth} = \bigoplus_{s=2}^{S} \hat{B}_{orth}^{s}, \tag{25}$$

the vector  $\tilde{\mathbf{z}}_{orth}^T = [\tilde{\mathbf{z}}_2^T, \dots, \tilde{\mathbf{z}}_S^T]$  is composed of S-1 vectors evolving independently of each other. (Each vector corresponds to a non-trivial irreducible representation of the graph automorphism group.) The stability of each block  $\hat{B}_{orth}^s$  depends on the largest real part of the eigenvalues of the block  $\lambda_{orth}^s$ , where the previously defined  $\lambda_{orth} \equiv \max_{s=2}^S \lambda_{orth}^s$ . This implies that for a given graph, certain clusters may achieve isolated group consensus while others may not, as shown in Example 2.

### VI. EXAMPLES

#### A. Example 1

We consider as an example the multilayer network with M=2 layers shown in Fig. 1. The state of the systems in the

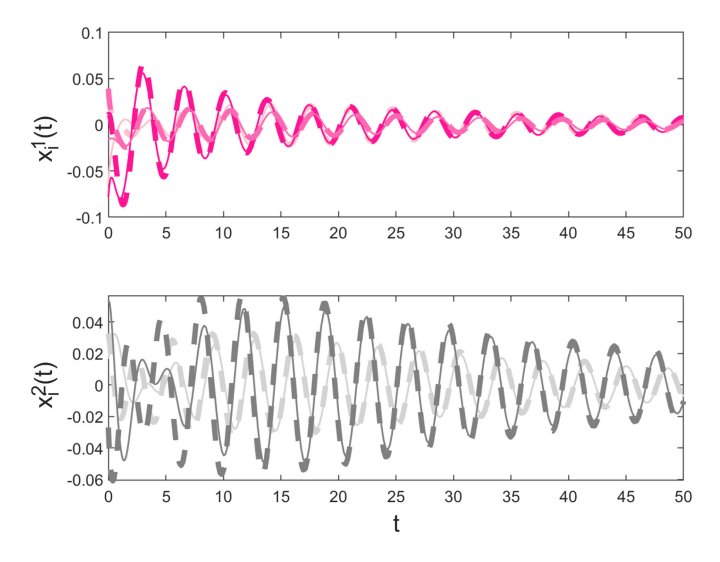


Fig. 2. Example of group consensus for a=2.4 and b=4.5. The upper plot shows the time traces from layer 1 and the lower plot shows the time traces from layer 2. Color of the time traces corresponds to the color of nodes shown in Fig. 1.

first layer is a scalar  $n^1 = 1$  while the state of the systems in the second layer is a two-dimensional vector  $n^2 = 2$ :

$$F^{1} = -3, \quad \hat{H}^{11} = 1, \quad \hat{H}^{12} = (0 - 1),$$

$$F^{2} = \begin{pmatrix} 0 & 1 \\ -b & -1 \end{pmatrix}, \quad \hat{H}^{21} = \begin{pmatrix} 0 \\ -a \end{pmatrix}, \quad \hat{H}^{22} = \begin{pmatrix} 0.1 & 0 \\ 0 & 0 \end{pmatrix}.$$
(26)

The quotient network is described by (17), where:

$$Q^{11} = \begin{bmatrix} 0 & 1 & 1 \\ 1 & 0 & 1 \\ 0 & 1 & 1 \end{bmatrix}, Q^{12} = Q^{21^T} = \begin{bmatrix} 1 & 0 \\ 0 & 1 \\ 0 & 0 \end{bmatrix}, Q^{22} = \begin{bmatrix} 1 & 2 \\ 2 & 0 \end{bmatrix}.$$
(27)

An example of group consensus corresponding to the case a=3.5 and b=4.5 is shown in Fig. 2. Shown are the time traces from layer 1 (top) and layer 2 (bottom). Colors of the time traces correspond to the colors of nodes shown in Fig. 1. The time traces corresponding to nodes in the same clusters from layer 1 and layer 2 converge to each other. However, nodes in different clusters converge following different time evolutions. The variety of dynamical behaviors that are observed by varying parameters a and b is shown in Fig. 2, where three cases are evidenced:

- I: stable dynamics and stable group consensus  $(\lambda_{para} < 0, \lambda_{orth} < 0)$
- II: unstable dynamics and stable group consensus  $(\lambda_{para} > 0, \lambda_{orth} < 0)$
- III: unstable dynamics and unstable group consensus  $(\lambda_{para} > 0, \lambda_{orth} > 0)$ .

The fourth possible case, stable dynamics and unstable group consensus, has not been observed when varying the parameters a and b in the range shown in Fig. 3.

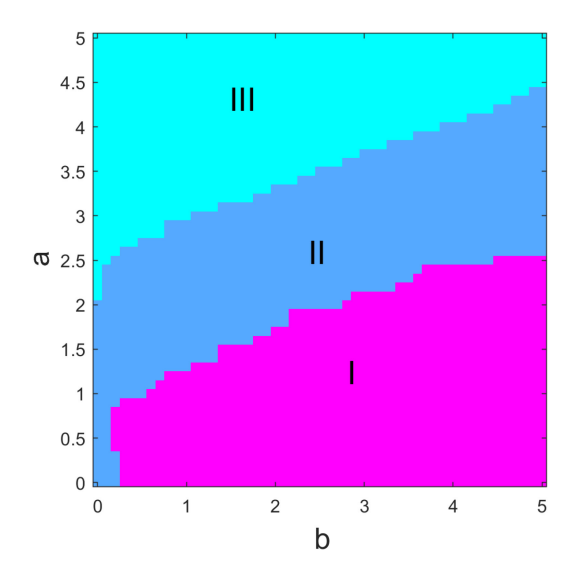


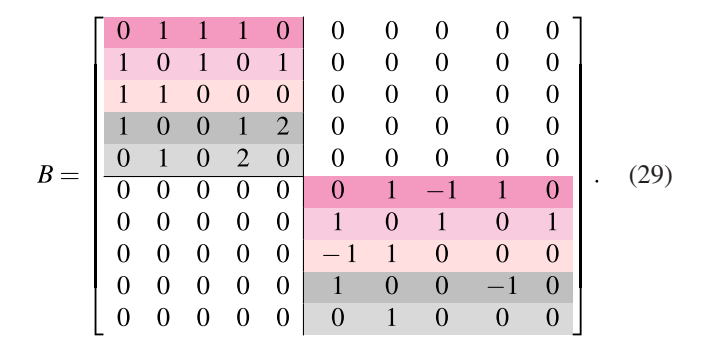
Fig. 3. Group consensus in the plane (a,b). I: stable dynamics and stable group consensus; II: unstable dynamics and stable group consensus; III: unstable dynamics and unstable group consensus.

The matrix T is equal to:

,	$\frac{1}{\sqrt{2}}$	0	$\frac{1}{\sqrt{2}}$	0	0	0	0	0	0	0
T =	0	$\frac{1}{\sqrt{2}}$	0	$\frac{1}{\sqrt{2}}$	0	0	0	0	0	0
	0	0	0	0	$\frac{1}{\sqrt{2}}$	$\frac{\frac{1}{\sqrt{2}}}{0}$	0	0	0	0
	0	0	0	0	0	0	$\frac{1}{\sqrt{2}}$	0	$\frac{1}{\sqrt{2}}$	0
	0	0	0	0	0	0	0	$\frac{\frac{1}{\sqrt{2}}}{0}$	0	$\frac{\frac{1}{\sqrt{2}}}{0}$
	$\frac{1}{\sqrt{2}}$	0	$-\frac{1}{\sqrt{2}}$	0	0	0	0	0	0	0
	0	$\frac{1}{\sqrt{2}}$	0	$-\frac{1}{\sqrt{2}}$	0	0	0	0	0	0
	0	0	0	0	$\frac{\frac{1}{\sqrt{2}}}{0}$	$-\frac{1}{\sqrt{2}}$	0	0	0	0
	0	0	0	0	0	Ó	$\frac{1}{\sqrt{2}}$	0	$-\frac{1}{\sqrt{2}}$	0
'	0	0	0	0	0	0	0	$\frac{1}{\sqrt{2}}$	o o	$-\frac{1}{\sqrt{2}}$
								•		(28)

Each row of the matrix T is colored to indicate a cluster of the multilayer network shown in Fig. 1: different shades of pink are clusters of layer 1; dark gray and light gray are clusters of layer 2. Hence, each row of the matrix T (and of the transformed matrix B) is associated with a specific cluster.

The matrix  $B = TAT^T$  is equal to:



In this case, there are only S=2 irreducible representations of the symmetry group: the matrix B has two diagonal blocks.

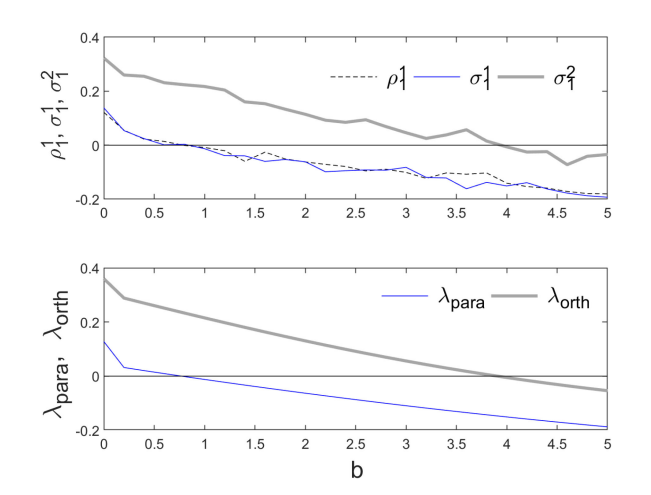


Fig. 4. Top:  $\rho^1_1$  (thick solid line),  $\sigma^1_1$  (thin solid line), and  $\sigma^2_1$  (thin dashed line), versus the parameter b for fixed a=2.4. Bottom:  $\lambda_{para}$  (thick solid line) and  $\lambda_{orth}$  (thin solid line), versus the parameter b.

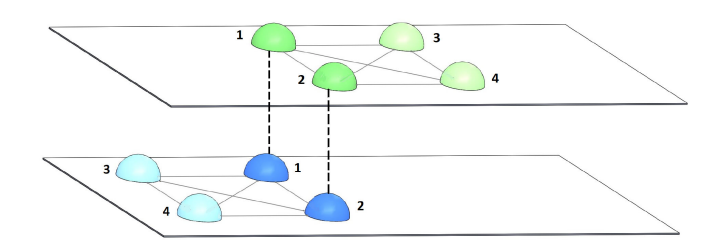


Fig. 5. A multilayer network with M=2 layers,  $N^1=4$  agents in layer 1 (top) and  $N^2=4$  agents in layer 2 (bottom). The agents in the top layer are of a different type than the agents in the bottom layer. Inside each layer, nodes in the same orbit (cluster) have the same color.

The upper-left diagonal block corresponds to motion parallel to the consensus manifold while the lower-right diagonal block corresponds to motion orthogonal to the consensus manifold

We define the average state for all the agents in cluster  $C_k^{\alpha}$  in layer  $\alpha$ :

$$[\mathbf{x}^{\alpha}(t)]_{k} = \frac{1}{N_{k}^{\alpha}} \sum_{j \in \mathcal{C}_{k}^{\alpha}} \mathbf{x}_{j}^{\alpha}(t)$$
 (30)

and compute the error  $E_j^{\alpha}(t)$  of node  $j \in \mathcal{C}_k$  with respect to the average trajectory:

$$E_j^{\alpha}(t) = \|\mathbf{x}_j^{\alpha}(t) - [\mathbf{x}^{\alpha}(t)]_k\|_2, \tag{31}$$

where  $j \in C_k^{\alpha}$ . We then compute the rates of exponential growth/decay:

$$\rho_k^{\alpha} = \frac{\log(\|[\mathbf{x}^{\alpha}(t_2)]_k\|) - \log(\|[\mathbf{x}^{\alpha}(t_1)]_k\|)}{t_2 - t_1}$$
(32)

and

$$\sigma_j^{\alpha} = \frac{\log(E_j^{\alpha}(t_2)) - \log(E_j^{\alpha}(t_1))}{t_2 - t_1}.$$
 (33)

Plot of  $\rho_1^1$  (thick solid line),  $\sigma_1^1$  (thin solid line), and  $\sigma_1^2$  (dashed line) versus the parameter b is shown in Fig. 4 (top).

Plot of the eigenvalues  $\lambda_{para}$  (solid line) and  $\lambda_{orth}$  (dashed line), versus the parameter b is shown in Fig. 4 (bottom). Note that  $\rho_1^1$  ( $\sigma_1^1$ ,  $\sigma_1^2$ ) is negative when the eigenvalue  $\lambda_{para}$  ( $\lambda_{orth}$ ) is negative.

### B. Example 2

We consider a multilayer network consisting of M=2 layers,  $N^1=4$  nodes in layer 1, and  $N^2=4$  nodes in layer 2, as shown in Fig. 5.

Matrices:

The state of the systems in both layers is two-dimensional  $(n^1 = n^2 = 2)$ :

$$F^{1} = \begin{pmatrix} -2 & 1 \\ -1 & -1 \end{pmatrix}, \quad \hat{H}^{11} = \begin{pmatrix} 1/3 & 0 \\ 0 & 1/3 \end{pmatrix}, \quad \hat{H}^{12} = \begin{pmatrix} 0 & -1 \\ 0 & 0 \end{pmatrix},$$

$$F^{2} = \begin{pmatrix} 0 & 1 \\ -2 & -2 \end{pmatrix}, \quad \hat{H}^{21} = -\hat{H}^{12^{T}}, \hat{H}^{22} = \begin{pmatrix} -a & 0 \\ 0 & 0 \end{pmatrix}.$$
(35)

The symmetry analysis shows that there are 2 clusters in layer 1:  $\mathcal{C}_1^1=(1,2), \mathcal{C}_2^1=(3,4)$  and 2 clusters in layer 2:  $\mathcal{C}_1^2=(1,2), \mathcal{C}_2^2=(3,4)$ . In Fig. 5, nodes in each layer have the same color if they belong in the same orbit (cluster).

The quotient network is described by (17), where:

$$Q^{11} = Q^{22} = \begin{bmatrix} 1 & 2 \\ 2 & 1 \end{bmatrix}, \quad Q^{12} = Q^{21}^T = \begin{bmatrix} 1 & 0 \\ 0 & 0 \end{bmatrix}.$$
 (36)

The matrix T is equal to:

$$T = \begin{pmatrix} \frac{1}{\sqrt{2}} & \frac{1}{\sqrt{2}} & 0 & 0 & 0 & 0 & 0 & 0 \\ 0 & 0 & \frac{1}{\sqrt{2}} & \frac{1}{\sqrt{2}} & 0 & 0 & 0 & 0 \\ 0 & 0 & 0 & 0 & \frac{1}{\sqrt{2}} & \frac{1}{\sqrt{2}} & 0 & 0 \\ 0 & 0 & 0 & 0 & 0 & 0 & \frac{1}{\sqrt{2}} & \frac{1}{\sqrt{2}} \\ \frac{1}{\sqrt{2}} & -\frac{1}{\sqrt{2}} & 0 & 0 & 0 & 0 & 0 \\ 0 & 0 & \frac{1}{\sqrt{2}} & -\frac{1}{\sqrt{2}} & 0 & 0 & 0 & 0 \\ 0 & 0 & 0 & 0 & \frac{1}{\sqrt{2}} & -\frac{1}{\sqrt{2}} & 0 & 0 \\ 0 & 0 & 0 & 0 & 0 & 0 & \frac{1}{\sqrt{2}} & -\frac{1}{\sqrt{2}} \end{pmatrix}.$$

$$(37)$$

Each row of the matrix T is colored to indicate a cluster of the multilayer network: dark green and light green are clusters of layer 1; dark blue and light blue are clusters of layer 2, see also Fig. 5.

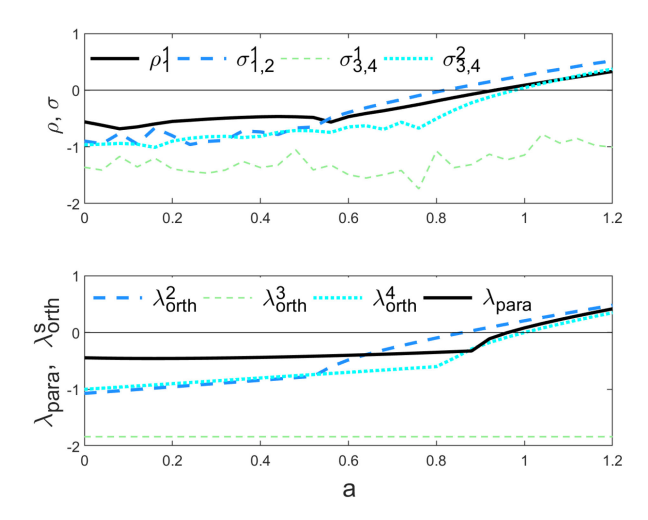


Fig. 6. Top:  $\rho_1^1$  (thick solid line),  $\sigma_{1,2}^1$  (thick dashed line, a similar plot is obtained for  $\sigma_{1,2}^2$ ),  $\sigma_{3,4}^1$  (thin dashed line),  $\sigma_{3,4}^2$  (thick dashed line) versus the parameter a. Bottom:  $\lambda_{para}$  (thick solid line),  $\lambda_{orth}^2$  (thick dashed line),  $\lambda_{orth}^3$  (thin dashed line), and  $\lambda_{orth}^4$  (thick dotted line) versus the parameter a.

The matrix  $B = TAT^T$ , after permutations of its rows/columns, is:

$$B = \begin{bmatrix} 1 & 2 & 1 & 0 & 0 & 0 & 0 & 0 & 0 \\ 2 & 1 & 0 & 0 & 0 & 0 & 0 & 0 & 0 \\ 1 & 0 & 1 & 2 & 0 & 0 & 0 & 0 & 0 \\ 0 & 0 & 2 & 1 & 0 & 0 & 0 & 0 & 0 \\ \hline 0 & 0 & 0 & 0 & -1 & 1 & 0 & 0 & 0 \\ 0 & 0 & 0 & 0 & 1 & -1 & 0 & 0 & 0 \\ 0 & 0 & 0 & 0 & 0 & 0 & -1 & 0 & -1 \end{bmatrix}$$
(38)

There are S=4 irreducible representations: the matrix Bhas four diagonal blocks. The upper-left diagonal block s=1corresponds to motion parallel to the consensus manifold while the remaining three diagonal blocks s = 2, 3, and 4correspond to motion orthogonal to the consensus manifold. Moreover, different from Example 1, these diagonal blocks correspond to various ways in which the group consensus state may be broken. The presence of multiple transverse blocks indicates the possibility of isolated group consensus in this network. The 2-dimensional s=2 block corresponds to simultaneous breaking of the dark green and dark blue clusters in Fig. 5. The largest real part of the eigenvalues of this block  $\lambda_{orth}^2$  determines group consensus of the cluster (1,2) in the top layer and of the cluster (1, 2) in the bottom layer. The two scalar blocks s=3 and s=4 correspond to independent breakings of the light green and light blue clusters, respectively. The largest real part of  $\lambda_{orth}^3$ , the eigenvalues of the s=3 block, determines group consensus of the cluster (3,4) in the top layer (light green cluster) while the largest real part of  $\lambda_{orth}^4$ , the eigenvalues of the s=4 block, determines group consensus of the cluster (3,4) in the bottom layer (light blue cluster).

Plots of  $\rho_1^1$ ,  $\sigma_{1,2}^1$ ,  $\sigma_{3,4}^1$ , and  $\sigma_{3,4}^2$  versus the parameter a are shown in Fig. 6 (top). As a increases, the first group consensus of the cluster (1,2) from the bottom layer (and, simultaneously, cluster (1,2) from the top layer) is lost. Then, the motion

parallel to the group consensus manifold becomes unstable. Finally, group consensus of the cluster (3,4) in the bottom layer is lost. Group consensus of the cluster (3,4) in the bottom layer is never lost. This is in agreement with the calculations of  $\lambda_{para}$ ,  $\lambda_{orth}^2$ ,  $\lambda_{orth}^3$ , and  $\lambda_{orth}^4$  shown in Fig. 6 (bottom). The possibility for some clusters to become unstable while other clusters remain stable, is *isolated group consensus*.

#### VII. CONCLUSIONS

We considered group consensus in multilayer networks based on their symmetries by transforming the network dynamics into a component parallel and components orthogonal to the group consensus manifold, which determine stability. Group consensus was predicted independently of the specific motion in the consensus manifold even when this motion is marginally stable or diverges. We demonstrated the applicability of the proposed method using two examples. For certain values of the parameters, the network may display isolated group consensus: some clusters are stable while others are not.

A case not considered in this paper is the group consensus arising from an equitable partition of the network nodes: a partition of the network nodes that is not predicted by the network symmetries [50]. An important direction for future investigation is to remove the assumption of undirected links, both in the inter-layer and in the intra-layer connections. We hope that our work will bring additional attention to the general topic of consensus and group consensus in multilayer networks.

## ACKNOWLEDGMENT

The authors thank Ms. Kiana Izadi for help in generating several figures in this paper. The author acknowledges the support of the Office of Naval Research through the Naval Research Laboratory's Basic Research Program.

## REFERENCES

- J. Yu and L. Wang, "Group consensus of multi-agent systems with undirected communication graphs," in *Proc. 7th Asian Control Conf.*, Hong Kong, SAR China, 2009, pp. 105–110.
- [2] J. Yu and L. Wang, "Group consensus in multi-agent systems with switching topologies and communication delays," Syst. Control Lett., vol. 59, no. 6, pp. 340–348, Jun. 2010.
- [3] J. Yu and L. Wang, "Group consensus of multi-agent systems with directed information exchange," *Int. J. Syst. Sci.*, vol. 43, no. 2, pp. 334–348, Feb. 2012.
- [4] J. Qin and C. Yu, "Group consensus of multiple integrator agents under general topology," in *Proc. 52nd IEEE Conf. Decis. Control*, Florence, Italy, 2013, pp. 2752–2757.
- [5] J. Qin, Q. Ma, H. Gao, Y. Shi, and Y. Kang, "On group synchronization for interacting clusters of heterogeneous systems," *IEEE Trans. Cybern.*, vol. 47, no. 12, pp. 4122–4133, Dec. 2017.
- [6] J. Qin, Q. Ma, W. X. Zheng, and H. Gao, "H∞ group consensus for clusters of agents with model uncertainty and external disturbance," in *Proc. 54th IEEE Conf. Decis. Control*, Osaka, Japan, 2015, pp. 2841–2846.
- [7] Y. Chen, J. Lü, F. Han, and X. Yu, "On the cluster consensus of discretetime multi-agent systems," Syst. Control Lett., vol. 60, no. 7, pp. 517–523, 2011
- [8] Y. Han, W. Lu, and T. Chen, "Cluster consensus in discrete-time networks of multiagents with inter-cluster nonidentical inputs," *IEEE Trans. Neural Netw. Learn. Syst.*, vol. 24, no. 4, pp. 566–578, Apr. 2013.
- [9] Y. Han, W. Lu, and T. Chen, "Achieving cluster consensus in continuoustime networks of multi-agents with inter-cluster non-identical inputs," *IEEE Trans. Autom. Control*, vol. 60, no. 3, pp. 793–798, Mar. 2015.

- [10] G.-S. Han, Z.-H. Guan, X.-M. Cheng, Y. Wu, and F. Liu, "Multiconsensus of second order multiagent systems with directed topologies," *Int. J. Control, Autom. Syst.*, vol. 11, no. 6, pp. 1122–1127, 2013.
- [11] J. Chen, M. Chi, Z.-H. Guan, R.-Q. Liao, and D.-X. Zhang, "Multiconsensus of second-order multiagent systems with input delays," *Math. Problems Eng.*, 424537, 2014.
- [12] J. Chen, Z.-H. Guan, T. Li, D.-X. Zhang, M.-F. Ge, and D.-F. Zheng, "Multiconsensus of fractional-order uncertain multi-agent systems," *Neurocomputing*, vol. 168, pp. 698–705, 2015.
- [13] J. Chen, Z.-H. Guan, D.-X. He, M. Chi, and X.-M. Cheng, "Multi-consensus for second-order multi-agent systems based on sampled position information," *IET Control Theory Appl.*, vol. 9, no. 3, pp. 358–366, 2015.
- [14] B. Hu, Z.-H. Guan, X.-W. Jiang, M. Chi, R.-Q. Liao, and C.-Y. Chen, "Event-driven multi-consensus of multi-agent networks with repulsive links," *Inf. Sci.*, vol. 373, pp. 110–123, 2016.
- [15] F. Sorrentino and E. Ott, "Network synchronization of groups," *Phys. Rev. E*, vol. 76, no. 5, 2007, Art. no. 56114.
- [16] C. R. S. Williams, T. E. Murphy, R. Roy, F. Sorrentino, T. Dahms, and E. Schöll, "Experimental observations of group synchrony in a system of chaotic optoelectronic oscillators," *Phys. Rev. Lett.*, vol. 110, no. 6, Feb. 2013, Art. no. 064104.
- [17] L. M. Pecora, F. Sorrentino, A. M. Hagerstrom, T. E. Murphy, and R. Roy, "Cluster synchronization and isolated desynchronization in complex networks with symmetries," *Nature Commun.*, vol. 5, no. 1, pp. 1–8, 2014.
- [18] F. Sorrentino, L. M. Pecora, A. M. Hagerstrom, T. E. Murphy, and R. Roy, "Complete characterization of the stability of cluster synchronization in complex dynamical networks," *Sci. Advances*, vol. 2, no. 4, 2016, Art. no. e1501737.
- [19] H.-X. Hu, W. Yu, G. Wen, Q. Xuan, and J. Cao, "Reverse group consensus of multi-agent systems in the cooperation-competition network," *IEEE Trans. Circuits Syst. I: Regular Papers*, vol. 63, no. 11, pp. 2036–2047, Nov. 2016.
- [20] H.-X. Hu, W. Yu, G. Wen, G. Qin, and Q. Cheng, in *Proc. 35th Chin. Control Conf.*, Chengdu, China, 2016, pp. 8302–8306.
- [21] Y. Gao, J. Yu, J. Shao, M. Yu, and Y. Gao, "Second-order group consensus in multi-agent systems with time-delays based on second-order neighbours' information," in *Proc. 34th Chin. Control Conf.*, Hangzhou, China, pp. 7493–7498.
- [22] Y. Feng, S. Xu, and B. Zhang, "Group consensus control for double-integrator dynamic multiagent systems with fixed communication topology," *Int. J. Robust Nonlinear Control*, vol. 24, no. 3, pp. 532–547, Feb. 2014.
- [23] I. Klickstein, L. Pecora, and F. Sorrentino, "Symmetry induced group consensus," *Chaos: An Interdisciplinary J. Nonlinear Sci.*, vol. 29, 2019, Art. no. 073101.
- [24] M. Kivela, A. Arenas, M. Barthélémy, J. P. Gleeson, Y. Moreno, and M. A. Porter, "Multilayer networks," *J. Complex Netw.*, vol. 2, no. 3, pp. 203–271, Aug. 2014.
- [25] S. Boccaletti et al., "The structure and dynamics of multilayer networks," Phys. Reports, vol. 544, no. 1, pp. 1–122, 2014.
- [26] F. D. Sahneh, C. Scoglio, and P. Van Mieghem, "Generalized epidemic mean-field model for spreading processes over multilayer complex networks," *IEEE/ACM Trans. Netw.*, vol. 21, no. 5, pp. 1609–1620, Oct. 2013.
- [27] F. D. Sahneh and C. Scoglio, "Competitive epidemic spreading over arbitrary multilayer networks," *Phys. Rev. E*, vol. 89, no. 6, 2014, Art. no. 062817.
- [28] E. Valdano, L. Ferreri, C. Poletto, and V. Colizza, "Analytical computation of the epidemic threshold on temporal networks," *Phys. Rev. X*, vol. 5, no. 2, 2015, Art. no. 021005.
- [29] M. De Domenico, C. Granell, M. A. Porter, and A. Arenas, "The physics of spreading processes in multilayer networks," *Nature Phys.*, vol. 12, no. 10, 2016, Art. no. 901.
- [30] H.-X. Hu, G. Wen, and W. X. Zheng, "Collective behavior of heterogeneous agents in uncertain cooperation-competition networks: A Nussbaum-type function based approach," *IEEE Trans. Control Netw. Syst.*, vol. 7, no. 2, pp. 783–796, Jun. 2020.
- [31] S. V. Buldyrev, R. Parshani, G. Paul, H. E. Stanley, and S. Havlin, "Catastrophic cascade of failures in interdependent networks," *Nature*, vol. 464, no. 7291, pp. 1025–1028, 2010.
- [32] J. Zhao, D. Li, H. Sanhedrai, R. Cohen, and S. Havlin, "Spatio-temporal propagation of cascading overload failures in spatially embedded networks," *Nature Commun.*, vol. 7, 2016, Art. no. 10094.
- [33] C. D. Brummitt, R. M. D'Souza, and E. A. Leicht, "Suppressing cascades of load in interdependent networks," *Proc. Nat. Acad. Sci.*, vol. 109, no. 12, pp. E680–E689, 2012.

- [34] M. De Domenico, A. Solé-Ribalta, E. Omodei, S. Gómez, and A. Arenas, "Ranking in interconnected multilayer networks reveals versatile nodes," *Nature Commun.*, vol. 6, 2015, Art. no. 6868.
- [35] F. Sorrentino, "Synchronization of a hypernetwork of coupled dynamical systems," *New J. Phys.*, vol. 14, 2012, Art. no. 033121.
- [36] D. Irving and F. Sorrentino, "Synchronization of a hypernetwork of coupled dynamical systems," *Phys. Rev. E*, vol. 86, 2012, Art. no. 056102.
- [37] W. He, G. Chen, Q.-L. Han, W. Du, J. Cao, and F. Qian, "Multiagent systems on multilayer networks: Synchronization analysis and network design," *IEEE Trans. Syst., Man Cybern.*: Syst., vol. 47, no. 7, pp. 1655–1667, 2017.
- [38] R. Sevilla-Escoboza, I. Sendiña-Nadal, I. Leyva, R. Gutiérrez, J. Buldú, and S. Boccaletti, "Inter-layer synchronization in multiplex networks of identical layers," *Chaos: An Interdisciplinary J. Nonlinear Sci.*, vol. 26, no. 6, 2016, Art. no. 065304.
- [39] I. Leyva, R. Sevilla-Escoboza, I. Sendiña-Nadal, R. Gutiérrez, J. Buldú, and S. Boccaletti, "Inter-layer synchronization in non-identical multilayer networks," Sci. Rep., vol. 7, 2017, Art. no. 45475.
- [40] K. A. Blaha, K. Huang, F. Della Rossa, L. Pecora, M. Hossein-Zadeh, and F. Sorrentino, "Cluster synchronization in multilayer networks: A fully analog experiment with LC oscillators with physically dissimilar coupling," *Phys. Rev. Lett.*, vol. 122, no. 1, 2019, Art. no. 014101.
- [41] P. Wang, G. Wen, X. Yu, W. Yu, and T. Huang, "Synchronization of multi-layer networks: From node-to-node synchronization to complete synchronization," *IEEE Trans. Circuits Syst. I: Regular Papers*, vol. 66, no. 3, pp. 1141–1152, Mar. 2019.
- [42] S. Lee and H. Shim, "Consensus of linear time-invariant multi-agent system over multilayer network," in *Proc. 17th Int. Conf. Control*, *Autom. Syst.*, 2017, pp. 133–138.
- [43] D. A. B. Lombana and M. Di Bernardo, "Multiplex pi control for consensus in networks of heterogeneous linear agents," *Automatica*, vol. 67, pp. 310–320, 2016.
- [44] C. G. Antonopoulos and Y. Shang, "Opinion formation in multiplex networks with general initial distributions," *Sci. Rep.*, vol. 8, no. 1, 2018, Art. no. 2852.
- [45] M. Golubitsky and I. Stewart, The Symmetry Perspective: From Equilibrium to Chaos in Phase Space and Physical Space. vol. 200, Berlin, Germany: Springer, 2003.
- [46] M. Tinkham, Group Theory and Quantum Mechanics. Courier Corporation, 2003.
- [47] F. Della Rossa, L. Pecora, K. A. Blaha, A. Shirin, I. Klickstein, and F. Sorrentino, "Cluster synchronization in multilayer networks with dependent and independent layer symmetries," to be published.
- [48] K. A. Blaha, K. Huang, F. Della Rossa, L. Pecora, M. Hossein-Zadeh, and F. Sorrentino, "Cluster synchronization in multilayer networks: A fully analog experiment with LC oscillators with physically dissimilar coupling" *Phys. Rev. Lett.*, vol. 122, no. 1, p. 014101, 2019.
- [49] M. T. Schaub, N. O'Clery, Y. N. Billeh, J.-C. Delvenne, R. Lambiotte, and M. Barahona, "Graph partitions and cluster synchronization in networks of oscillators," *Chaos: An Interdisciplinary J. Nonlinear Sci.*, vol. 26, no. 9, 2016, Art. no. 94821.
- [50] A. B. Siddique, L. Pecora, J. D. Hart, and F. Sorrentino, "Symmetry-and input-cluster synchronization in networks," *Phys. Rev. E*, vol. 97, no. 4, 2018 Art. no. 42217.



Francesco Sorrentino (Member, IEEE) received the master's degree in industrial engineering and the Ph.D. degree in control engineering both from the University of Naples Federico II, Naples, Italy, in 2003 and 2007, respectively. His expertise is in dynamical systems and controls, with particular emphasis on nonlinear dynamics and adaptive decentralized control. His work includes studies on dynamics and control of complex dynamical networks and hypernetworks, adaptation in complex systems, sensor adaptive networks, coordinated autonomous

vehicles operating in a dynamically changing environment, and identification of nonlinear systems. He is interested in applying the theory of dynamical systems to model, analyze, and control the dynamics of complex distributed energy systems such as power networks and smart grids. Subjects of current investigation are evolutionary game theory on networks (evolutionary graph theory), the dynamics of large networks of coupled neurons, and the use of adaptive techniques for dynamical identification of communication delays between coupled mobile platforms. He has authored more than 50 papers in international scientific peer reviewed journals.



Louis Pecora received the B.S. degree in physics from Wilkes College, Wilkes-Barre, PA, USA, in 1969. After two years of graduate work with Purdue University and a year as a foreman with the Hazleton Weaving Company. He received the Ph.D. degree in solid state science program from Syracuse University, Syracuse, NY, USA, in 1977. He is currently a Research Physicist with the Naval Research Laboratory, Washington, DC, USA where he heads the section for Magnetic Materials and Nonlinear Dynamics in the Materials and Sensors branch. His dissertation

topics included the effects of adsorbed gases on the magnetic properties of fine iron particles and correlations between metallic properties and atomic electronic states in transition metals. In 1977, he was awarded an NRC Postdoctoral Fellowship with the Naval Research Laboratory where he worked on applications of positron annihilation techniques in determining electronic states in copper alloys. This led to a permanent position at NRL in 1979 with continuation of the positron work into areas of reconstruction of momentum densities using novel tomographic techniques in collaboration with the international group at the University of Geneva. In the mid-1980's, He moved into the field of nonlinear dynamics in solid state systems. Early work led to the discovery and characterization of chaotic transients in spin-wave behavior in yttrium iron garnets. Subsequent work has focused on the applications of chaotic behavior, especially the effects of driving systems with chaotic signals. This has resulted in the discovery of synchronization of chaotic systems, control and tracking, dynamics of many coupled, and nonlinear systems. Recently, his research interests have turned to quantum chaos. He has authored more than 150 scientific papers and has five patents for the applications of chaos. His original paper on the synchronization of chaotic systems has over 6000 (ISI) citations and is the 10th most cited paper ever in *Physical Review Letters*. He is a Fellow of the AAAS and the American Physical Society.



Ljiljana Trajkovic (Fellow, IEEE) received the Dipl. Ing. degree from the University of Pristina, Pristina, Yugoslavia, in 1974, the M.Sc. degrees in electrical engineering and computer engineering from Syracuse University, Syracuse, NY, USA, in 1979 and 1981, respectively, and the Ph.D. degree in electrical engineering from University of California at Los Angeles, Los Angeles, CA, USA, in 1986.

She is currently a Professor with the School of Engineering Science, Simon Fraser University, Burnaby, BC, Canada. From 1995 to 1997, she was a

National Science Foundation Visiting Professor with the Electrical Engineering and Computer Sciences Department, University of California, Berkeley, Berkeley, CA, USA. She was a Research Scientist with Bell Communications Research, Morristown, NJ, USA from 1990 to 1997, and a Member of the Technical Staff at AT&T Bell Laboratories, Murray Hill, NJ, USA from 1988 to 1990. Her research interests include high-performance communication networks, control of communication systems, computer-aided circuit analysis and design, and theory of nonlinear circuits and dynamical systems.

Dr. Trajković serves as IEEE Division X Delegate/Director (2019–2020) and served as IEEE Division X Delegate-Elect/Director-Elect (2018). She served as Senior Past President (2018-2019), Junior Past President (2016-2017), President (2014-2015), Vice President Publications (2012-2013, 2010–2011), and a Member at Large of the Board of Governors (2004–2006) of the IEEE Systems, Man, and Cybernetics Society. She served as 2007 President of the IEEE Circuits and Systems Society and a member of its Board of Governors (2004-2005, 2001-2003). She is Chair of the IEEE Circuits and Systems Society joint Chapter of the Vancouver/Victoria Sections. She was Chair of the IEEE Technical Committee on Nonlinear Circuits and Systems (1998). She is General Co-Chair of SMC 2020 and SMC 2020 Workshop on BMI Systems and served as General Co-Chair of SMC 2019 and SMC 2018 Workshops on BMI Systems, SMC 2016, and HPSR 2014, Special Sessions Co-Chair of SMC 2017, Technical Program Chair of SMC 2017 and SMC 2016 Workshops on BMI Systems, Technical Program Co-Chair of ISCAS 2005, and Technical Program Chair and Vice General Co-Chair of ISCAS 2004. She served as an Associate Editor for the IEEE Transactions on Cir-CUITS AND SYSTEMS (Part I) (2004-2005, 1993-1995) and (Part II) (2018, 2002-2003, 1999-2001), and the IEEE CIRCUITS AND SYSTEMS MAGAZINE (2001-2003). She is a Distinguished Lecturer of the IEEE Systems, Man, and Cybernetics Society (2020-2021) and the IEEE Circuits and Systems Society (2010–2011, 2002–2003). She is a Professional Member of IEEE-HKN.